NON-DARCIAN SEEPAGE EQUILIBRIUM ANALYSIS OF SPLITTING GROUTING FLUID IN SMOOTH SINGLE FRACTURE

by

***Pei-Tao QIU*[a], *Xiao-Jun YANG*[b,c,*], *Hai PU*[c,d]**

[a]School of Civil Engineering, Xuzhou University of Technology, Xuzhou 221018, China
[b]State Key Laboratory for Geo-Mechanics and Deep Underground Engineering, China University of Mining and Technology, Xuzhou 221116, China
[c] School of Mathematics, China University of Mining and Technology, Xuzhou 221116, Jiangsu, China
[d]College of Mining Engineering and Geology, Xinjiang Institute of Engineering, Urumqi, Xinjiang, 830091, China

In this paper, the slurry seepage dynamics model is established, the critical conditions for instability of the seepage dynamics model are discussed, and the effects of power index, effective mobility and non-Darcian flow factors on the seepage velocity are analyzed. The results show that in the two-dimensional logarithmic parameter space, the boundary between the stability zone and the instability zone of seepage is a straight line, and the absolute value of the slope of the straight line decreases with the increase of the power index.

Key words: *seepage instability, fracture grouting, non-Darcian, non-Newtonian*

Introduction

With the wide application of grouting engineering, the theory of grouting reinforcement has been continuously developed and improved [1-3]. Due to the diversity of the proportion and working conditions of grouting materials, which often involve solid mechanics, fluid mechanics, rock mechanics and other disciplines [4-7]. It is difficult to make theoretical research, which leads to the phenomenon that the development of grouting theory has been lagging behind practice. The grouting theory is mainly divided into seepage grouting, compaction grouting and splitting grouting [8]. Seepage grouting and compaction grouting are regarded as homogeneous fluid. Considering its diffusion in rock and soil fractures, the diffusion forms of grout mainly include spherical and cylindrical diffusion theories [9-10]. Cleavage grouting is to increase the grouting pressure to cause the rock and soil mass to have a cleavage channel, and greatly increase the amount of grouting to improve the support effect [11].

Permeation grouting is conducted at low pressure, which is not easy to cause

[*] Corresponding author; e-mail: dyangxiaojun@163.com

damage to soil structure. It is often used to improve the impermeability and strength index of rock and soil mass [12]. Many scholars have improved the theory of seepage grouting from the aspects of grouting material type, slurry viscosity, slurry setting time, stratum type, stratum permeability coefficient, soil porosity, grouting pressure and grouting hole diameter, etc., from the gradual evolution of seepage diffusion based on the classical Marguerite theory to the consideration of grout injectability, fluidity, time-varying and percolation [13-14]. The research of compaction grouting theory mainly focuses on the grouting mechanism. The basic mechanical principle is the expansion model of column hole (vertical or horizontal) and spherical hole based on elastoplastic theory or strain stress relationship. In the process of research, it is gradually found that the maximum grouting pressure and the pore water pressure, effective stress, water pressure dissipation caused by the pressure filtration effect should be considered. In the latest research, the effective influence range of compaction grouting has been proposed [15-16]. The research results of split grouting theory focus on the soil compactness, water content, grouting pressure, grouting hole depth, etc. In the analysis of grouting mechanism, the slab narrow slit model, the plane radial circle model, the induced directional splitting, the influence of major and minor principal stresses, and the theory of circular hole expansion are mainly considered [17-19]. Since the essence of splitting grouting is to compact the soil mass, compared with seepage grouting and compaction grouting, it can form splitting cracks and grout vein skeleton in the soil mass, with a larger reinforcement range and better effect. Therefore, it is of great significance to study the limit equilibrium state of the grout seepage process during splitting grouting to guide the engineering reinforcement practice.

In this paper, considering that the two-phase fluid of grouting slurry belongs to non-Newton fluid, a slurry seepage dynamic model of the two-phase medium in rock soil structure is established. Based on the assumptions, the boundary conditions and initial conditions of the model are given, the critical conditions for the instability of the model are discussed, and the effects of power index, effective mobility and non-Darcy flow factors on the seepage velocity are analyzed.

Seepage model for Non-Newtonian fluid in a smooth fissure

In the process of high-pressure fracturing grouting, due to the large velocity of the slurry, the Reynolds coefficient of the slurry is large. At this time, the influence of inertial force must be considered. The seepage velocity and pressure gradient do not meet the Darcy's law. In addition, the slurry used in high-pressure fracturing grouting shows obvious characteristics of non-Newtonian fluid, that is, the shear stress is nonlinear with the angular strain rate. Therefore, to analyze the structural instability of fractured rock mass under high pressure, the following assumptions should be made for the actual engineering problems.

(1) The seepage force at both ends of slurry seepage under high pressure can drive slurry particles to roll or move between pores.

(2) The slurry is a continuous medium filled uniformly in the water body, and its seepage characteristics meet the Forchheimer relation.

(3) The slurry is a non-Newtonian fluid, meeting the characteristics of power-law fluid, i.e. $\tau = C\gamma^n$ (when $n < 1$ is a pseudoplastic fluid, and $n > 1$ is an expansive fluid), where, C is the slurry consistency coefficient, and n is a power index.

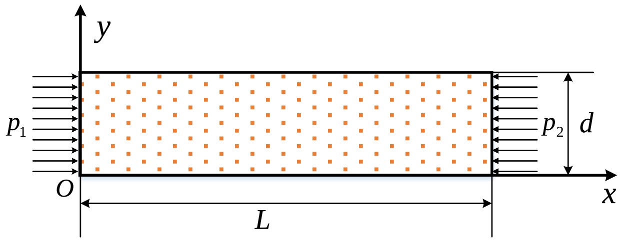

Fig. 1Schematic diagram of slurry seepage dynamic model

Based on the above basic assumptions, a dynamic model as shown in Figure 1 can be established. The stability of seepage is composed of the mass conservation equation, momentum conservation equation and fluid compression equation of non-Darcian flow slurry in smooth parallel seepage channels, that is to say,

$$\frac{\partial \rho}{\partial t}+\frac{\partial(\rho \upsilon)}{\partial x}=0 \tag{1-a}$$

$$\rho c_a \frac{\partial \upsilon}{\partial t}=-\frac{\partial p}{\partial x}-\frac{\mu_e}{k_e}\upsilon^n-\rho\beta\upsilon^2 \tag{1-b}$$

$$\rho=\rho_0\left[1+c_f\left(p-p_0\right)\right] \tag{1-c}$$

where p is pressure, υ is seepage velocity, ρ is mass density of mixed liquid, μ_e is equivalent viscosity, is k_e effective permeability, β is non-Darcian flow β factor, c_f is fluid compressibility coefficient, p_0 is standard atmospheric pressure, and ρ_0 is mass density of fluid under standard atmospheric pressure. The effective permeability and equivalent viscosity are determined by the width of seepage channel b and the constitutive parameters of Non Darcian fluid reads

$$k_e=\frac{b^2}{12n} \tag{2}$$

$$\mu_e=\frac{C}{n}\left(\frac{6}{b}\right)^{n-1} \tag{3}$$

The boundary conditions of the dynamic model is written as

$$p\big|_{x=0}=p_1 \tag{4-a}$$

and

$$p\big|_{x=L}=p_2 \tag{4-b}$$

The initial conditions for pressure and velocity are showed as follows:

$$p\big|_{t=0}=p_1+\frac{p_2-p_1}{L}x, x\in\left[0,L\right] \tag{5-a}$$

and

$$\upsilon\big|_{t=0}=\upsilon_{st} \tag{5-b}$$

When the slurry seepage dynamics model is in equilibrium, the density, velocity and pressure at both ends of the slurry do not change with time, that is $\partial\rho/\partial t=0$, $\partial\upsilon/\partial t=0$ and $\partial p/\partial t=0$. If the slurry is regarded as an incompressible fluid, the equilibrium state of the slurry seepage dynamics model is given by the following equations:

$$\frac{\partial \upsilon}{\partial x} = 0, \frac{\mu_e}{k_e}\upsilon^n + \rho\beta\upsilon^2 + \frac{p_2 - p_1}{L} = 0, p = p|_{t=0} \tag{6}$$

Let

$$f(\upsilon) = \frac{\mu_e}{k_e}\upsilon^n + \rho\beta\upsilon^2 + \frac{p_2 - p_1}{L}.$$

Using Runge_kutta method can get that the nonzero root of the algebraic equation $f'(\upsilon) = 0$ is given as

$$\upsilon^* = \left(-\frac{2\rho I_e \beta}{n}\right)^{\frac{1}{n-2}} \tag{7}$$

where $I_e = k_e / \mu_e$ is called the effective mobility.

When $f(\upsilon^*) < 0$, the function $f(\upsilon)$ has a zero point and the seepage velocity has a stable value; When $f(\upsilon^*) < 0$, function $f(\upsilon)$ has no zero point, that is, the second equation in expression (6) has no real root. At this time, no matter what the initial conditions are, the seepage cannot reach the equilibrium state, and the seepage is unstable. Therefore, by substituting equation (7) into $f(\upsilon^*) < 0$, it can be obtained that the instability conditions of slurry seepage dynamic model can be written as follows:

$$\rho\beta\left(-\frac{2\rho\beta I_e}{n}\right)^{\frac{2}{n-2}} + \frac{1}{I_e}\left(-\frac{2\rho\beta I_e}{n}\right)^{\frac{n}{n-2}} - \frac{p_1 - p_2}{L} < 0 \tag{8}$$

If $n < 2$, (8) is further simplified by taking logarithms on both sides, and the boundary line between the stable zone and the unstable zone of seepage can be expressed as:

$$\frac{2}{n}\ln\left(I_e^*\right) + \ln\left(-\beta^*\right) = -\ln\left(\frac{2\rho}{n}\right) + \frac{n-2}{n}\ln\left(\frac{2}{2-n}\frac{p_1 - p_2}{L}\right) \tag{9}$$

The linear solution is the limit case of seepage equilibrium state, as shown in Figure 2, which gives the limit seepage equilibrium state of several special fluids.

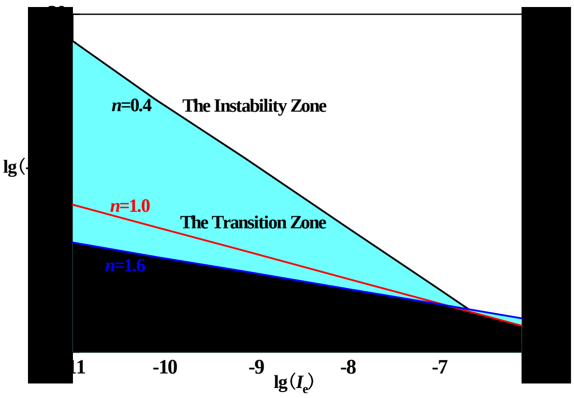

Fig.2 Power law fluid seepage critical instability curve

The main physical and mechanical parameters of the seepage dynamic model in the figure are set in Table 1. The power exponent n is 0.4, 1.0 and 1.6, respectively, for pseudo plastic fluid, Newtonian fluid and expansive fluid.

Table 1. Main physical and mechanical parameters of seepage dynamic model

L (m)	ρ (g/cm^3)	p_1 (MPa)	p_2 (MPa)	c_a (%)
0.25	1.92	0.70	0.04	3.96×10^4

It can be seen from Figure 2 that the power index n, effective mobility I_e and non-Darcy flow β factor determine the existence of seepage equilibrium. After the power index n is determined, under the two-dimensional logarithmic parameter space (I_e,β), the boundary line between the stable and unstable areas of seepage is a straight line, and the absolute value of the slope of the straight line decreases with the increase of the power index. When the point determined in the parameter space (I_e,β) is below the straight line, the fluid is always in equilibrium, otherwise, the seepage loss is stable.

Seepage equilibrium analysis

It can be seen from the discussion of chapter 3 that the stability of non-Darcian flow in non-Newtonian fluids in smooth cracks is jointly determined by three parameters. Two of them are parameters that characterize non-Newtonian fluids (power exponent n, effective fluidity I_e) and one that characterizes non-Darcian flow characteristics (non-Darcy flow β factor). Therefore, the analysis of the seepage equilibrium state of chapter 4 selects three parameters of power exponent n, effective fluidity I_e and non-Darcian flow β factor to study their effects on seepage velocity.

Effect of power exponent on seepage velocity

In order to obtain the influence of the power exponent on the velocity under steady state of seepage, we set the effective fluidity $I_e = 7.00\times10^{-8}\,\mathrm{m}^{3.3}\mathrm{s}^{0.7}/\mathrm{kg}$, non-Darcian flow factor $\beta = 1.10\times10^4\,\mathrm{m}^{-1}$, the power exponents were taken at 0.3, 0.7, 1.0, 1.3, and 1.6 to observe the change of seepage velocity.

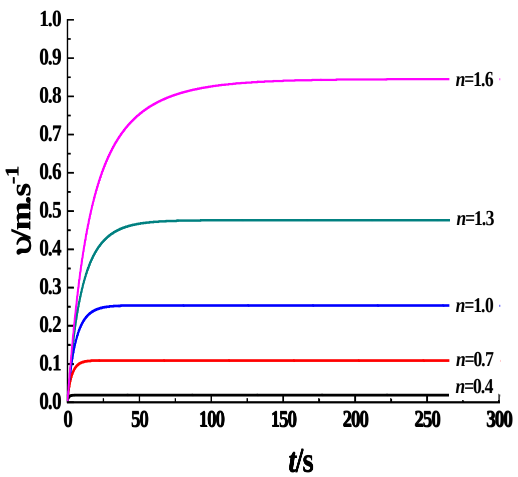

Fig.3 Seepage velocity curve with time under different power exponents

It can be seen from Fig. 3 that in the case of a certain power exponent, the seepage velocity increases with time, and finally the percolation velocity tends to a fixed value, no longer changes with time, and the seepage reaches a steady state.

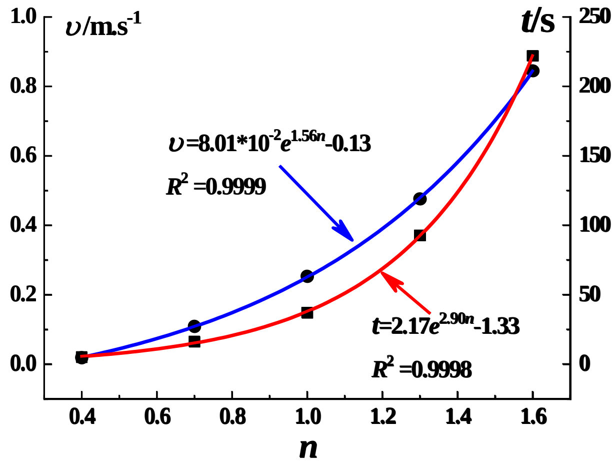

Fig.4 The time required for stable seepage velocity and seepage steady state with power exponential curve

It can be seen from Fig. 4 that the steady seepage velocity increases with the increase of the power exponent, and the slope increases continuously. This relationship can be better characterized by an exponential function $\upsilon = 8.01\times10^{-2}e^{1.56n} - 0.13$.

Effect of effective fluidity on seepage velocity

In order to obtain the effect of effective fluidity on the velocity under steady seepage, we set the power exponent $n = 1.3$, non-Darcian flow factor $\beta = 1.10\times10^4$ m^{-1}, the effective fluidity were taken at 0.5×10^{-8} $\mathrm{m^{3.3}s^{0.7}/kg}$, 1.0×10^{-8} $\mathrm{m^{3.3}s^{0.7}/kg}$, $3.0\times10^{-8}\mathrm{m^{3.3}s^{0.7}/kg}$, $5.0\times10^{-8}\mathrm{m^{3.3}s^{0.7}/kg}$ and $7.0\times10^{-8}\mathrm{m^{3.3}s^{0.7}/kg}$ to observe the change of seepage velocity.

It can be seen from Fig. 5 that in the case of a certain effective fluidity, the percolation velocity increases with time, and finally the percolation velocity tends to a constant value and reaches a steady state.

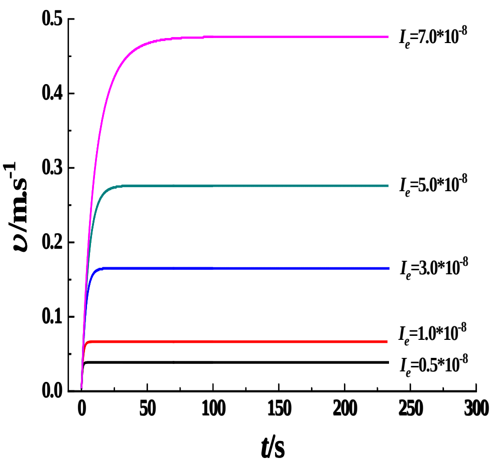

Fig.5 Seepage velocity curve with time under different effective fluidity

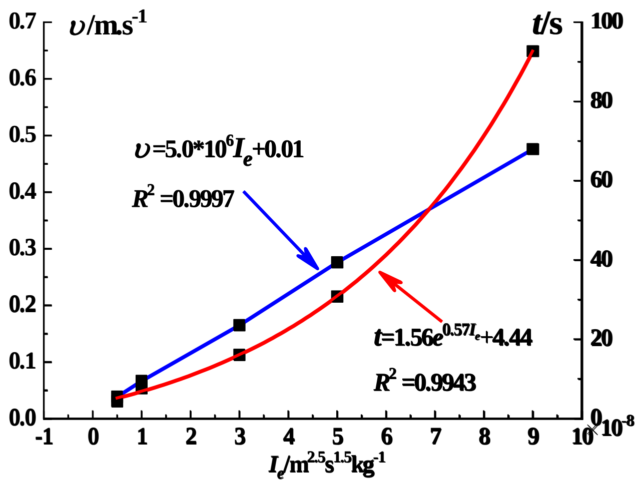

Fig.6 The time required for stable seepage velocity and seepage steady state with effective fluidity curve

It can be seen from Fig. 6 that the steady seepage velocity increases with the increase of the effective fluidity, and this relationship can be better characterized by $\upsilon = 5.0 \times 10^6 I_e + 0.1$.

Effect of non-Darcian flow factor on seepage velocity

In order to obtain the effect of non-Darcian flow factor on the velocity under steady seepage, we set the power exponent $n = 1.3$, effective fluidity $I_e = 7.00 \times 10^{-8}\,\mathrm{m}^{3.3}\mathrm{s}^{0.7}/\mathrm{kg}$, the non-Darcian flow factor were taken at $0.3 \times 10^4\,\mathrm{m}^{-1}$, $0.5 \times 10^4\,\mathrm{m}^{-1}$, $0.7 \times 10^4\,\mathrm{m}^{-1}$, $0.9 \times 10^4\,\mathrm{m}^{-1}$ and $1.1 \times 10^4\,\mathrm{m}^{-1}$ to observe the change of seepage velocity.

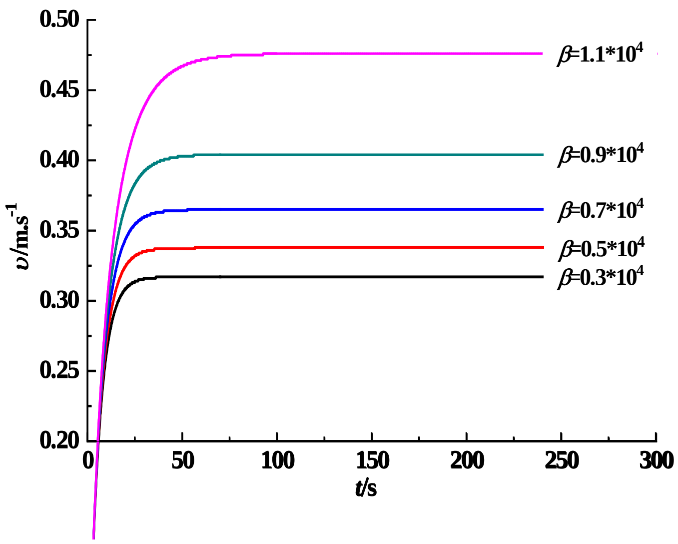

Fig.7 Seepage velocity curve with time under different non-Darcian flow factor

It can be seen from Fig. 7 that in the case of a certain non-Darcian flow β factor, the seepage velocity increases with time, and finally the percolation velocity tends to a constant value and reaches a steady state.

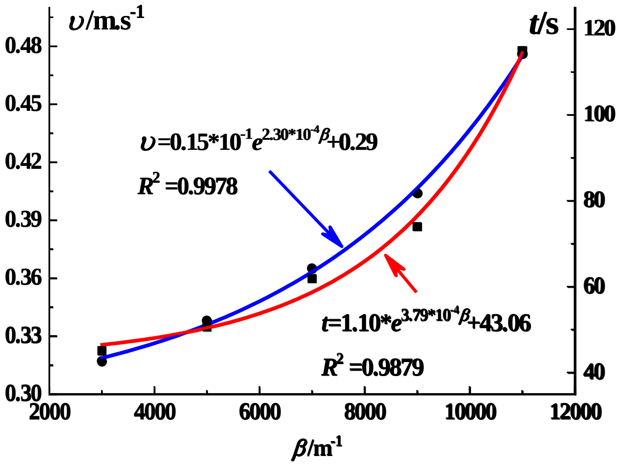

Fig.8 The time required for stable seepage velocity and seepage steady state with non-Darcian flow factor curve

It can be seen from Fig. 8 that the steady seepage velocity tends to increase with the increase of the non-Darcian flow factor, and the slope becomes larger and larger. This relationship can be better characterized by an exponential function $\upsilon = 1.50\times 10^{-2} e^{2.30\times 10^{-4}\beta} + 0.29$.

Conclusion

In this work we have studied the seepage stability of high-pressure fracturing grouting for strengthening engineering structures with cracks. The slurry seepage dynamics model is established, the critical conditions for instability of the seepage dynamics model are discussed, and the effects of power index, effective mobility and non-Darcian flow factors on the seepage velocity are analyzed. The results show that in the two-dimensional logarithmic parameter space, the boundary between the stability zone and the instability zone of seepage is a straight line, and the absolute value of the slope of the straight line decreases with the increase of the power index. The velocity and time required for seepage stability are positively correlated with power index, effective mobility and non-Darcian flow factor, which can be better described by exponential function. With the increase of the power index, the sensitivity of the fluid to the pressure response gradually increases, which shows that the seepage acceleration increases and the time required for stability increases. The greater the mobility, the stronger the fluid flow capacity and the longer the time required for seepage stability. The greater the non-Darcian flow factor is, the greater the slope of seepage velocity increase and the more deviated from Darcy flow.

Acknowledgement

This work was supported by the National Science Foundation of China (51974296), General Project of Basic Science (Natural Science) Research in Jiangsu Universities (22KJB130014)，University-level Science and Technology Cultivation Project of XZIT (XKY2019115).

Nomenclature

L —broken rock particle size,[m]

c_a —acceleration coefficient,[%]

ρ_0 —mass density of fluid,[g/cm^3]

p_1 —left boundary pressure value,[MPa]

p_2 —right boundary pressure value,[MPa]

ρ —mass density of the mixture,[g/cm^3]

k_e —effective permeability,[m/s]

υ —seepage velocity,[m/s]

μ_e —dynamic viscosity,[$\mathrm{Pa \cdot s}$]

β —non-Darcian flow factor,[m^{-1}]

References

[1] Zhang, Q. S.,*et al.*, Dynamic Alteration Behavior ofGranite under SC-CO_2: Proposal for a Long termAccelerated Test Method, *Bulletin of Engineering Geology and the Environment*, *81* (2022), 335,pp. 1-16

[2] Li, S. C., *et al.*, Prediction for Water Inrush Disaster Source and CFD-Based Design of Evacuation Routes in Karst Tunnel, *International Journal of Geomechanics*,5 (2022), 22,pp. 1-12

[3] Xu, C. Y., *et al.*, Investigation on Artificial Boundary Problem in the Combined Finite-discrete Element Method (FDEM), *Computers and Geotechnics*, 4 (2022), 151,pp.1-16

[4] Wu, J. Y.,*et al.*, Effects of Carbon Nanotube Dosage and Aggregate Size Distribution on Mechanical Property and Microstructure of Cemented Rockfill, *Cement and Concrete Composites*, 2 (2022), 127,pp.1-21

[5] Ma, G., *et al.*, Experimental and Numerical Investigations on Fracture Behaviours of Cracked Chevron Notched Brazilian Disc (CCNBD) Sandstone Specimen under Cyclic Loading, *Engineering Fracture Mechanics*, 2022,271, August, 108673

[6] Yang, X. J., *et al.*, *General Fractional Derivatives with Applications in Viscoelasticity*, Academic Press, New York, USA, 2020

[7] Wu, J. Y., *et al.*, Particle Size Distribution of Aggregate Effects on Mechanical and Structural Properties of Cemented Rockfill: Experiments and Modeling, *Construction and Building Materials*, 5 (2018), 193, pp.295-311

[8] Niu, J. D., *et al*.,Experimental Study of Split Grouting Reinforcement Mechanism in Filling Medium and Effect Evaluation, *Sensors*, 11 (2020), 20,pp.1-19

[9] Wang, K., *et al*., Understanding the Effect of Cementitious Grouting Pressure on Micro-Fracture Permeability for Rock Reinforcement Underground: A Lab Study, *Energies*, 13 (2020), 16, pp.1-15

[10] Dai, C. Q., *et al.*, Development and Engineering Application of Strong Permeability Grouting Material for Weathered Granite Formation, *Revista Romana De Materiale-Romanian Journal of Materials*, 3 (2019), 49, pp.379-387

[11] Cheng, W. C., *et al*., Modeling of Permeation and Fracturing Grouting in Sand: Laboratory Investigations, *Journal of Testing and Evaluation*, 5 (2018), 46, pp.2067-2082

[12] Karytsas, S., *et al*., Barriers Against and Actions Towards Renewable Energy Technologies Diffusion: A Principal Component Analysis for residential ground source heat pump (GSHP) systems, *Renewable and Sustainable Energy Reviews*,78 (2017), pp.252-271

[13] Peng, M., *et al*., Recent Advances in the GPR Detection of Grouting Defects behind Shield Tunnel Segments, *Remote Sensing*, 22 (2021), 13, pp.1-21

[14] Jorne, F., *et al*., Evaluation of the Grout Injectability and Types of Resistance to Grout Flow, *Construction and Building Materials*, 122 (2016), pp.171-183

[15] Shi, H., *et al*., Physical Test of Fracture Development in the Overburden Strata above the Goaf and Diffusion Process of Permeable Grout Slurry, *Bulletin of Engineering Geology*

and the Environment, 6 (2021), 80, pp.4791-4802
[16] Hong, K. R., *et al*., Typical Underwater Tunnels in the Mainland of China and Related Tunneling Technologies, *Engineering*, 6 (2018), 3, pp.871-879
[17] Yun, J. W., *et al*., Cement-based Fracture Grouting Phenomenon of Weathered Granite Soil, *Ksce Journal of Civil Engineering*, 1 (2017), 21, pp.232-242
[18] Li, Z., *et al*., Grouting Effect on Rock Fracture Using Shear and Seepage Assessment, *Construction and Building Materials*, 242 (2020), pp.1-16
[19] Guo, Y. X., *et al*., Grouting Rock Fractures under Condition of Flowing Water, *Carbonates and Evaporites*, 3 (2020), 35, pp.1-15

Paper submitted: September 6, 2022
Paper revised: October 10, 2022
Paper accepted: November 12, 2022